

NMR Screening Applied to the Fragment-Based Generation of Inhibitors of Creatine Kinase Exploiting a New Interaction Proximate to the ATP Binding Site

Anne-Sophie Bretonnet,[†] Anne Jochum,[‡] Olivier Walker,[†] Isabelle Krimm,[†] Peter Goekjian,[‡] Olivier Marcillat,[§] and Jean-Marc Lancelin^{*,†}

Laboratoire de RMN et Spectrométrie de Masse Biomoléculaires, Université Claude Bernard Lyon 1, UMR CNRS 5180 Sciences Analytiques, ESCPE Lyon, Laboratoire de Chimie Organique II-Glycochimie, Université Claude Bernard Lyon 1, UMR CNRS 5181 Méthodologie de Synthèse et Molécules Bio-Actives, ESCPE Lyon, and Biomembranes et Enzymes Associés, UMR CNRS 5246, Université Claude Bernard Lyon 1, 69622 Villeurbanne, France

Received December 21, 2006

Using an in-house fragment NMR library, we identified a set of ligands that bind rabbit muscular creatine kinase, an enzyme involved in key ATP-dependent processes. The ligands docked to the crystal structures of creatine kinase indicated that a phenylfuroic acid could enter into a pocket adjacent to the nucleotide binding site. This fragment served as an anchor to develop in silico a series of potential inhibitors which could partly access the nucleotide binding site. The short synthesis of only four derivatives provided entirely novel hit compounds that reversibly inhibit creatine kinase at micromolar concentrations with a mixed ATP-competitive/noncompetitive mechanism in agreement with the structural model of the inhibited enzyme. These initial biologically active compounds are novel and modular and exploit a new interaction proximate to the ATP binding site.

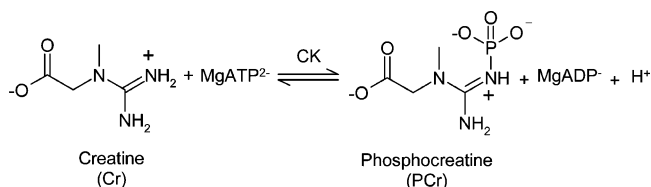
Introduction

Identifying an initial biologically active compound for a new target protein (hit compound)¹ either for drug discovery or as a pharmacological tool remains a troublesome step. Considerable progress has been made in the route from hit to clinical candidate, including early integration of ADMET parameters,¹ new computational and chemical methods have already been successfully tested,² and a few NMR-based methods have raised particular interest along this line.^{3–5} However, widely used approaches for hit generation, including high-throughput screening (HTS), natural product leads, structural analogy to existing inhibitors, or rational design, are not appropriate in a number of situations.

Small molecular fragments have therefore gained widespread popularity as a tool for drug design and hit generation over the past decade. Fragments have simple features, which differ from those of the more elaborate “leadlike” or “druglike” properties of combinatorial compounds.⁶ Fragments are thus more readily amenable to chemical modifications, and have a higher probability of binding protein targets.⁷ Hence, fragment libraries can be much smaller than HTS libraries while sampling a chemical space inaccessible to the latter, sometimes disclosing binding “needles” where HTS would fail to find hits.⁸

A set of empirical rules have been established that define the proper features for a fragment to allow tractable optimization.⁹ Those limits, known as the “rule of three”¹⁰ ($M_w \leq 300$ g·mol⁻¹, H bond donors and acceptors <3, rotatable bonds <3, and polar surface area ≤ 60 Å²), usually restrict the affinities of fragments within the micro- to millimolar range. These affinities are unsuitable for detection by classical HTS methods, but are typical of those dealt with by NMR methods^{11,12} or other structural techniques. The combined power of both structural methods and fragment concepts makes the approach particularly

Scheme 1. Interconversion of Creatine to Phosphocreatine Catalyzed by Creatine Kinase in the Presence of MgATP



viable. The capacity to generate an initial biologically active “hit” compound with a minimal number of biological tests is attractive in cases which are not amenable to broad screening. Furthermore, some structural information may be obtained which can be valuable for guiding further inhibitor design. Finally, the hits generated by fragment-based design are of high quality: the inhibitors are modular, water-soluble, and simple, and are thus more readily developed into lead compounds or pharmacological tools.

Diverse collections of compounds (from a few dozen¹³ to hundreds^{14,15} or even thousands^{16,17}) have previously been gathered in accordance with various criteria to perform NMR screening.¹⁸ Importantly, known drug scaffolds can be used as fragment templates to minimize toxicity and untractability issues in further drug design.^{19,20} This underpinned a pioneering work by Fejzo et al. where a 100-compound library called SHAPES was used to identify several ligands of the p38 MAP kinase and inosine-5'-monophosphate dehydrogenase.¹⁵

Using an approach similar to SHAPES, we developed an in-house NMR library of just 53 compounds and tested it with established NMR screening protocols on rabbit muscle creatine kinase (RMCK; EC 2.7.3.2).²¹ This enzyme plays multiple roles in the cellular energy distribution network²² by catalyzing the reversible transfer of a phosphate group between adenosine triphosphate (ATP) and creatine (Cr; Scheme 1). It is interesting as a model system for phosphagen kinases such as brain creatine kinase and arginine kinase, both potential targets for new drugs,^{23,24} because RMCK is commercially available and compatible with NMR requirements (buffer, temperature, ex-

* To whom correspondence should be addressed. E-mail: lancelin@hikari.cpe.fr. Phone/fax: 0033 472 431 395.

[†] Laboratoire de RMN et Spectrométrie de Masse Biomoléculaires.

[‡] Laboratoire de Chimie Organique II-Glycochimie.

[§] Biomembranes et Enzymes Associés.

periment time). We describe herein the NMR screening and a fragment evolution strategy against this enzyme that enabled us to design and synthesize novel hit inhibitors. These scaffolds exploit a new binding site in proximity of the nucleotide binding site, and could be useful for future design of lead molecules to refine the current knowledge about RMCK and related homologues.²⁵

Results and Discussion

Compound Selection and NMR Tests. Initially 61 SHAPES-like commercial compounds were dissolved in DMSO-*d*₆ stock solutions and tested for aqueous solubility and purity by ¹H NMR spectra.²⁶ WaterLOGSY (water ligand observed via gradient spectroscopy) spectra were used to detect possible aggregation, as large LOGSY effects are characteristic of high molecular weight compounds in water.²⁷ From this preliminary study, a fraction of the initial set of compounds were withdrawn from the library owing to poor aqueous solubility (six compounds) or chemical instability (one compound) or because their signals were partially suppressed with that of water (one compound). A few compounds showed limited but still practical solubility in either DMSO-*d*₆ or H₂O and were thus used at their highest practical concentrations as stock solutions in their best solvent. The 53 stock solutions were finally tested for stability at +4 °C, and no degradation was detectable over a year.

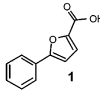
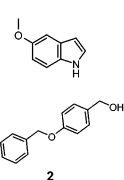
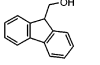
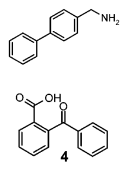
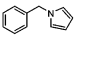
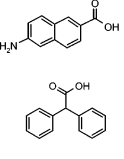
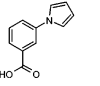
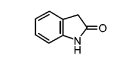
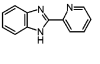
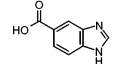
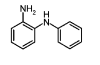
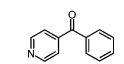
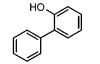

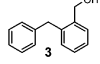
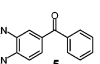
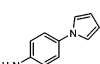
Affinity Screening of Rabbit Muscular Creatine Kinase. RMCK was first tested with one of its endogenous ligands, adenosine diphosphate complexed to Mg²⁺ (MgADP). NMR saturation transfer difference (STD) spectra confirmed the affinity of CK for the nucleotide. Using this NMR method, we found a dissociation constant (*K*_D) in the micromolar range (*K*_D = 300 ± 40 μM at 20 °C; see the Experimental Section). This is slightly higher than the 70 ± 13 μM previously reported from enzymatic data,²¹ but still of the same order of magnitude. It should be noted here that NMR titrations have already previously been found to somewhat overevaluate dissociation constants.²⁸

The NMR screening library was tested against CK. A total of 19 compounds out of 53 were qualitatively retained as possible weak-to-good ligands (Table 1) on the basis of their STD and LOGSY effects (see for instance Figure 1). Among the NMR hits, phenylfuroic acid (**1**) displayed the highest STD amplification factor (see the Experimental Section) and the highest LOGSY effect and was therefore titrated precisely against CK. Its dissociation constant was millimolar (*K*_D = 5 mM ± 1 mM, Figure 2), and no direct competition with MgADP was evidenced by adding increasing and saturating amounts of MgADP. This suggests that MgADP and **1** do not share the same binding site. One may thus be driven to a fragment evolution strategy in which **1**, correctly linked with another ligand of even moderate affinity for the nucleotide site, would form a tight-binding ligand owing to the additive strength of the two moieties.^{5,29}

Structural Insights. Docking of the NMR Hits. Docking simulations can give valuable insight into the structures of the CK complexes evidenced by NMR. The program DOCK 5.4³⁰ was used to confirm and complement our first data, using RMCK structural models (see the Experimental Section).

The active site of CK is known to undergo a significant conformational change when bound to its substrates, creatine and MgATP.³¹ This was particularly clear in the recent X-ray structure of the *Torpedo californica* dimer,³² where each subunit was unexpectedly crystallized in different conformations: one

Table 1. Selected Ligands Detected by NMR and Their STD and LOGSY Effects

Ligand ^a	<i>f</i> _{STD} ^b	LOGSY effect ^b	Ligand ^a	<i>f</i> _{STD} ^b	LOGSY effect ^b
	5.1	200%		2.4	90%
	3.3	100%		1.9	158%
	3.2	69%		1.8	62%
	3.1	120%		1.4	14%
	3.0	127%		1.3	35%
	3.0	39%		1.3	0%
	2.8	142%		1.3	0%
	2.8	83%			
	2.5	41%			
	2.5	nd ^c			

^a The ligand concentration was 1 mM and the CK concentration was 5 or 10 μM for STD and WaterLOGSY measurements, respectively. ^b STD amplification factors (*f*_{STD}) and LOGSY effects were calculated as described in the Experimental Section. ^c Not determined.

“open”, substrate-free, and one “closed” with a transition-state analogue of the Cr-ATP adduct. Two flexible loops in particular (namely, from residues 59–69 and 322–331) moved 20 Å closer to each other upon substrate binding. Thus, the conformational changes of CK cannot be reasonably anticipated when fragments enter the large groove of the active site. Hence, our study was systematically performed on both the open and closed enzymes as detailed in the Experimental Section.

Fragment **1** is the best fragment in terms of binding energy. In closed and open structures, **1** was docked in a specific site located between those of creatine and the nucleotide (MgADP, MgATP), with the phenyl ring directed toward the nucleotide pocket (Figure 3a). This result is in accordance with the NMR experiments since no direct competition could be evidenced between **1** and MgADP. Addition of diverse substituents to the phenyl ring of **1**, to access the nucleotide binding site, thus seemed an appropriate follow-up strategy.

In Silico Follow-Up of CK Ligands. A total of 1000 follow-up compounds of **1**, complying with the Lipinski rules for druglike compounds,³³ were randomly generated. They all consisted of a common moiety, **1**, extended from its phenyl ring using various fragment structures and linker types (see Table 2). The linkers were either *meta* or *para* to the furan ring of **1**. Those follow-ups were systematically docked to RMCK. They were then classified to identify the best follow-up characteristics, in terms of the positions and types of substituents and linkers.

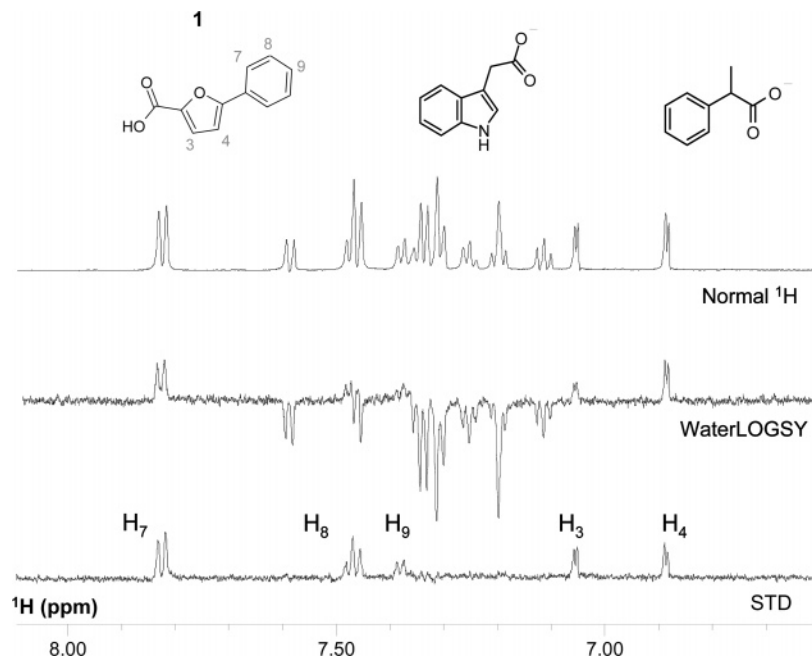


Figure 1. Identification of **1** as a hit fragment among a mixture with two other compounds of the fragment library (middle and right formulas) by NMR screening. WaterLOGSY and STD experiments both confirm the affinity of **1** for the protein target, CK: the peaks for compound **1** are the higher LOGSY effect (200%) and the only peaks in the STD spectrum.

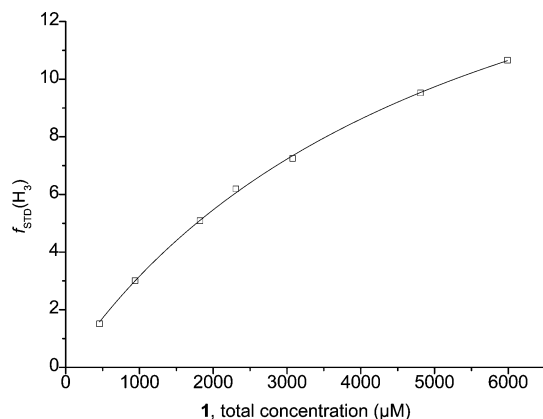


Figure 2. Binding curve of compound **1** from STD experiments in the presence of 10 μM CK at 20 °C. Concentrations are plotted against STD amplification factors (f_{STD}) to determine the dissociation constant K_D (5 ± 1 mM).

An analysis of the 250 top-ranked compounds enabled us to propose the following features: (i) three preferred substituent structures were represented almost exclusively, fragments **2**, **3**, and then **4** and other derivatives of the benzophenone type, such as **5**, in decreasing order (see Table 2); (ii) two-atom linkers were preferred, and among those, the amide linker was the most frequent; (iii) *meta* and *para* substitutions of the phenyl ring were equally well represented. Thus, the type of linker and substitution position seemed to be less important than the substituent with regard to the calculated binding energy of the fragment-designed molecules. These substituents interact with residues in the phosphate and adenosine pockets of the ATP binding site.

As a consequence, archetypal fragment-based molecules with potentially optimal affinities could be proposed for synthesis. From many possible combinations those with benzophenone substituents were preferred, owing to their commercial availability and their chemical tractability in a minimal number of steps. Since DOCK especially predicted ligand **5** in the

nucleotide binding site, this compound might be a good candidate as a follow-up substituent. As a result, molecules **10a–c** were selected, and their syntheses were carried out according to Scheme 2a. An additional compound without the amide linker, molecule **11**, was also synthesized from another route detailed in Scheme 2b.

Chemical Syntheses. The substituted phenylfuroic acids were prepared by Suzuki coupling between a furoic acid derivative and an appropriate substituted phenylboronic acid (Scheme 2). The basic conditions of the Suzuki coupling required the protection of the carboxylic acid with an acid-labile group such as a *tert*-butyl ester. Thus, ester **6**³⁴ reacted with 4-carboxyphenylboronic acid to afford the acid **7** in good yield.³⁵ The carboxylic acid **7** was activated with oxalyl chloride in the presence of a catalytic amount of DMF to yield the acyl chloride **8**,³⁶ which was reacted with different amines to obtain amides **9a–c**. Subsequent hydrolysis of the *tert*-butyl ester with trifluoroacetic acid provided the corresponding acids **10a–c** (Scheme 2a).³⁷

Compound **11** was synthesized via a Suzuki coupling between 5-(4-bromophenyl)-2-furoic acid and 4-benzoylphenylboronic acid³⁵ (Scheme 2b).

NMR Assay of the Candidate Inhibitors. Molecule **10a** was the most amenable to NMR testing owing to its high (millimolar) solubility in aqueous phosphate buffer. It was thus tested as a first potential inhibitor by NMR, and its ¹H spectrum clearly showed a significant line broadening upon addition of CK (Figure 4a). This feature typically indicates a rapid to intermediate exchange of the molecule between a complexed and a free form on the NMR time scale. The high affinity of **10a** for CK was confirmed and characterized by STD and WaterLOGSY spectra in the presence of MgADP. Indeed the affinity of MgADP was significantly reduced when **10a** was added, giving rise to a sign change in the WaterLOGSY spectrum (not shown) and to a drop in intensity in the STD spectrum (Figure 4b). This change can be used to evaluate the K_D of **10a** for CK, assuming a direct competition between **10a** and MgADP by

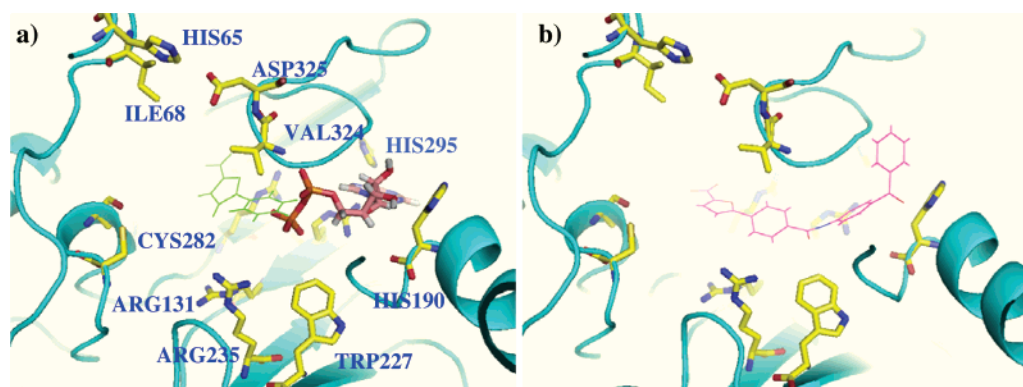
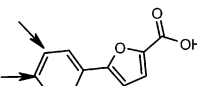
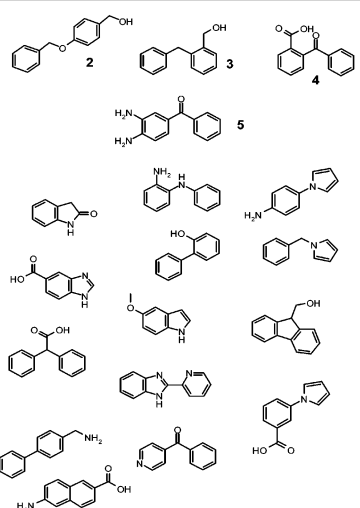
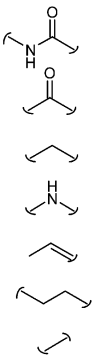
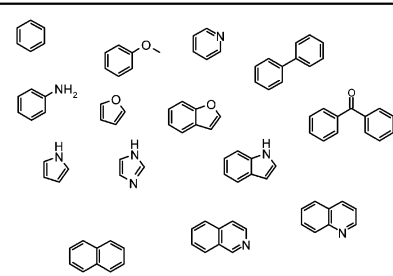


Figure 3. (a) Binding site of compound **1** (green sticks) modeled by docking calculations on the closed form of CK. ADP (red sticks) is represented in the vicinity of **1** as well as the major residue side chains involved in catalysis (yellow sticks). (b) Lowest energy model of molecule **10a** docked to the active site of RMCK.

Table 2. In Silico Design of Follow-Ups^a

(Substituent) + Linker 		
Substituents : other ligands from screen	Linkers :	+ Restrictions :
		M _w < 500 g/mol -3 < clogP < 5 H-bond acceptors ≤ 10 H-bond donors ≤ 5 1 ≤ cycles ≤ 4
+Additional scaffolds :		
		
↓ ↓ ↓ 1 000 follow-up molecules		

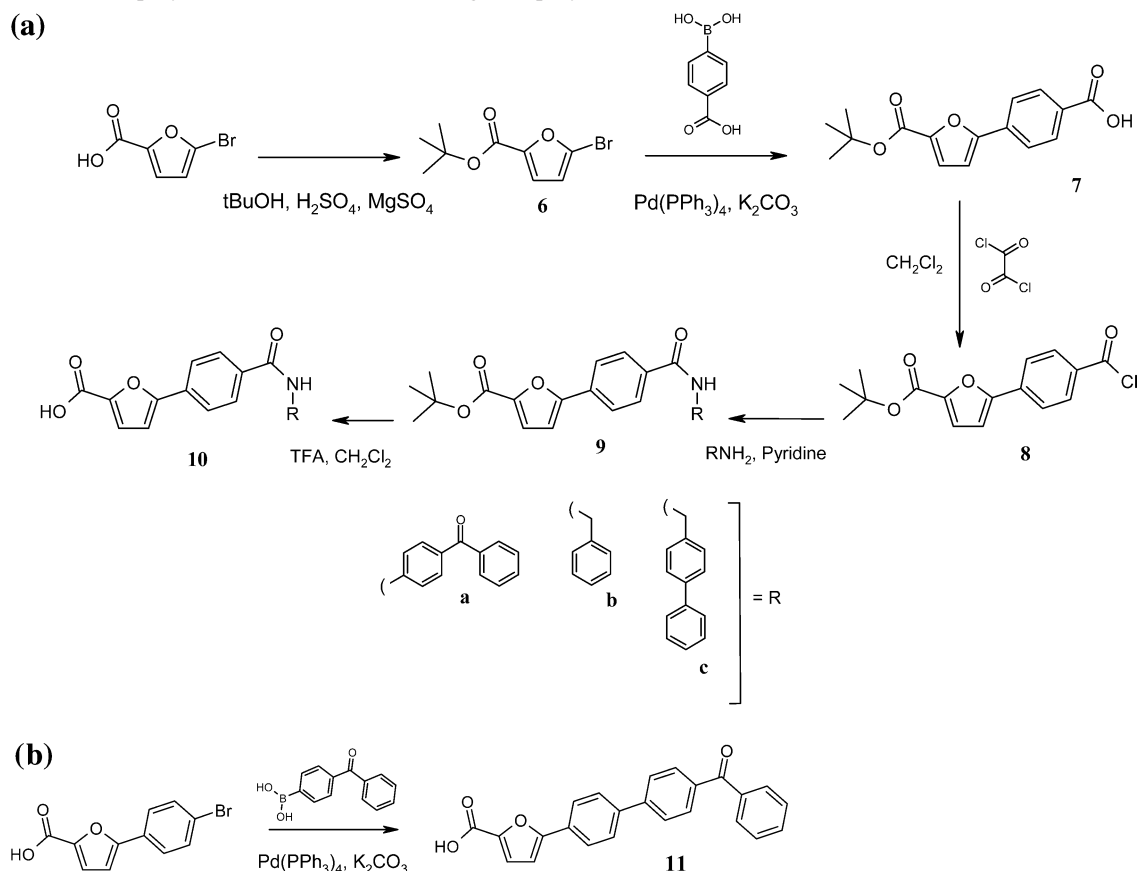
^a Different fragment substituents (left column) are appended to the initial ligand (compound **1**, top row). Different linkers were used (middle column), and several restrictions were applied to select a total of 1000 appropriate follow-ups.

using the formula³⁸

$$K_D^{10a} = [10a] \frac{K_D^{ADP}(1 - i)}{i(K_D^{ADP} + [ADP])}$$

where [10a] and [ADP] are the concentrations of **10a** and ADP, respectively, K_D^{ADP} is the dissociation constant of the CK–

MgADP complex ($K_D^{ADP} = 300 \pm 40 \mu\text{M}$ from NMR), and i is decrease of the STD signal in the presence of **10a** relative to the same signal without **10a**. With an average 38% decrease of the STD signals of ADP (initially at $500 \mu\text{M}$) in the presence of **10a** (at $250 \mu\text{M}$) this leads to an approximate dissociation constant of $150 \mu\text{M}$. The significant affinity of **10a** for CK, and its effect on the binding of MgADP, was subsequently

Scheme 2. (a) Five-Step Synthesis of **10a–c** and (b) Single-Step Synthesis of **11**.

confirmed next by an enzymatic assay on **10a** as well as on the other follow-up compounds.

Enzymatic Assays. Residual enzymatic activity in the presence of increasing **10a** concentrations has been measured in standard pH-stat assay conditions with 4 mM ATP and 40 mM creatine to evaluate the inhibitor concentration giving 50% inhibition (IC_{50}). The results, plotted as the ratio of the reaction rate in the presence of **10a** versus the rate in its absence, are shown in Figure 5a, which suggest an IC_{50} in the 50 μ M range. We noticed that inhibition is progressive (steady state is reached 3 min after inhibitor addition; for all measurements, the enzyme was thus incubated with **10a** and creatine for 3 min, and reaction was started by addition of ATP). Creatine kinase intrinsic fluorescence is known to be attenuated by the nucleotide substrate binding,³⁹ but due to its high UV absorption coefficient, **10a** is responsible for a strong inner filter effect which precludes a quantitative analysis of its binding through fluorescence measurements.

Reversibility of the inhibition was assessed by measuring the reaction rate at constant substrates and inhibitor concentrations but with different enzyme concentrations. A plot of the reaction rate versus enzyme concentration shows that, with or without **10a**, the reaction rate increases linearly with the amount of enzyme added to catalyze the reaction, the slope decreasing in the presence of **10a** (not shown), as expected for a reversible inhibitor.

The kinetics of ATP hydrolysis has been followed, as described in the Experimental Section, with or without **10a** (27.5 and 55 μ M) with constant amounts of CK and creatine. Reaction rates were best fitted to an equation describing a mixed type of reversible inhibition⁴⁰ (Figure 5b). The $1/v$ versus $1/[ATP]$ plot (Figure 5c) shows the characteristic pattern expected for this type of inhibition. Variation of K_{ATP} and V_m with **10a** concen-

tration allowed us to calculate the two constants $K_I = 25 \pm 5 \mu$ M and $\alpha K_I = 70 \pm 4 \mu$ M, which respectively describe binding of **10a** on free enzyme and on the enzyme–MgATP complex. These values are somewhat lower than those extrapolated from NMR measurements, but this is quite commonly observed.²⁷ A more complete analysis of CK reaction inhibition by **10a** would also require analysis of reaction rates with variable creatine concentration; these measurements have not been done here.

All the follow-up molecules were next assayed using a single concentration of MgATP, and their inhibitory properties were compared to those from a reference experiment, performed with no inhibitor. A ranking of all molecules could thus be established on the basis of their inhibitory properties expressed as a percentage of the reference activity (Table 3). From this ranking, two molecules (**10c** and **11**) appear as the best inhibitors, both inhibiting CK by 63%. On the other hand, molecule **10b** only has a weak 20% inhibitory effect.

Structural Insights. Docking of the Inhibitors. Using the same protocols as for the first fragments, molecules **10a–c** and **11** were docked to the structural models of the closed RMCK. A ranking of the molecules according to their docking energies was in good agreement with the experimental results (Table 3) except for molecule **11**, the docking energy of which was underestimated by DOCK. Figure 3b shows the lowest energy model for **10a**, confirming the competition between this molecule and MgADP for the same binding site. Indeed, molecule **10a** adopts an elongated conformation in which the benzophenone moiety makes significant contacts with the nucleotide binding site. An analysis of ligand–protein contacts (LPCs) derived with LPC software⁴¹ showed that **10a** interacts with Arg129, Arg235, and Arg291, all important and conserved residues for phosphate chain stabilization, and His190, which is involved in adenosine stabilization.³² Molecule **10b**, having

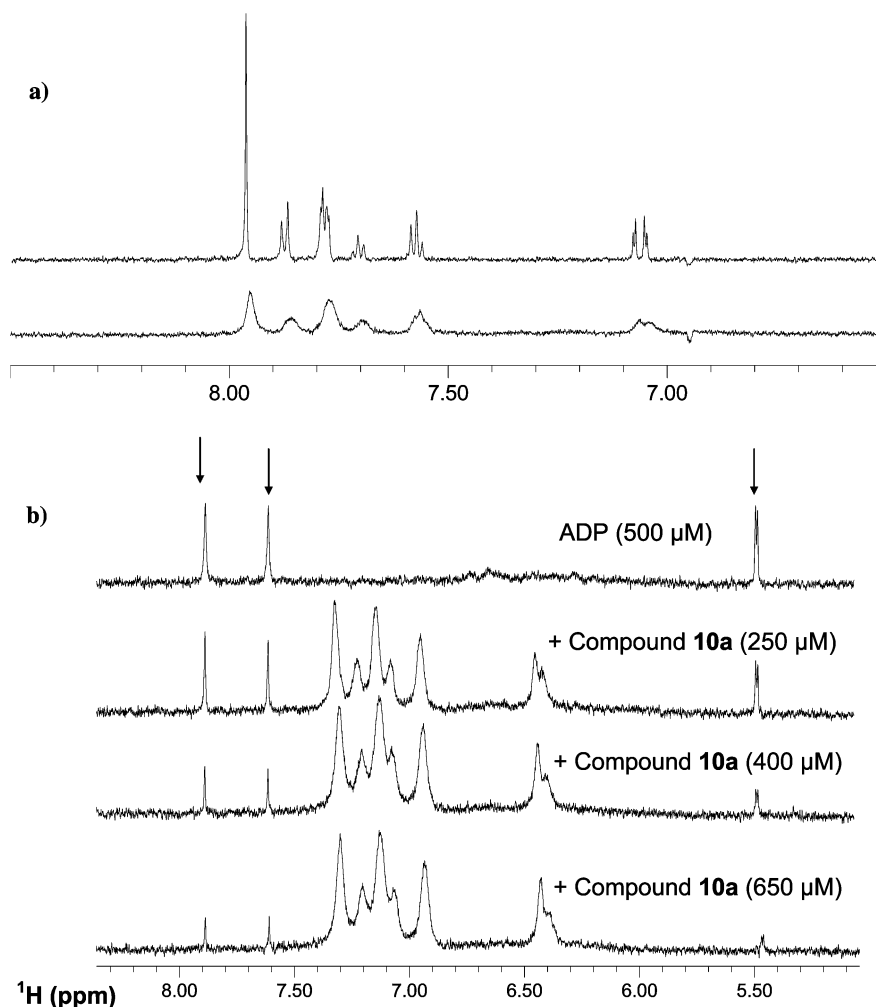


Figure 4. (a) Aromatic regions of the ¹H spectra of compound **10a** at 100 μM in the absence (top trace) and presence (bottom trace) of 10 μM CK. Line broadening is clearly apparent, showing that **10a** is interacting with CK. (b) STD spectra of ADP in the absence (top trace) and presence (other traces) of increasing amounts of **10a**. ADP resonances are marked with an arrow.

a less bulky substituent than other inhibitors, also has less contact in the nucleotide pocket, and this could explain its lower inhibitory properties. More importantly, the furoic acid moiety of **10a–c**, analogous to fragment **1**, is docked at a position similar to that of the initial compound **1**. Assuming that this subsite is potentially accessible in CK, either in the presence or in the absence of MgATP, this could explain the mixed competitive/noncompetitive inhibition mechanism evidenced for **10a**.

Concluding Remarks

We have demonstrated that a minimum fragment library (ca. 50 molecules) could be used in conjunction with NMR to develop micromolar inhibitors of RMCK on the basis of the synthesis of only a very limited number of compounds. With molecular modeling and docking, the hit fragments were readily extrapolated to fully new, non-nucleotide reversible inhibitors evidenced to act in a mixed competition/noncompetition mode against MgATP. The docked models confirm that the inhibitors interact in part with the ATP/ADP–Mg binding site. The molecular features of the new hit compounds can now be used as novel bases for designing more active and selective inhibitors of creatine kinase, or related isozymes of the guanidinium kinase family, such as arginine kinase, which is involved in several infectious diseases.^{24,42}

Experimental Section

Library Collection. The compounds (at least 95% pure) were chosen from Aldrich or Acros online catalogs, using their substructure search facilities combined with SHAPES-like selection criteria inspired from published lists.^{15,19,20,43} The chosen compounds had to fit the rule of three;¹⁰ to this effect, partition coefficients either experimental or calculated were obtained using the KowWin software (Syracuse Research Corp.).⁴⁴ Whenever documented, aqueous solubility was also taken into account since millimolar concentrations were ideally sought in the final samples.

Stock Solutions of CK for NMR and Enzymatic Assays. RMCK was purchased from Roche (reference 10 127 566 001) as a lyophilized, ATPase-free powder. A single stock solution at 26 mg/mL (300 μM dimeric CK) was prepared from each new batch in phosphate-buffered H₂O (50 mM, pH 6.8, and 0.02% NaN₃ to prevent microbial growth). It was dispatched in 550 μL aliquots, conserved at –30 °C between uses. Enzymatic activity was not affected by serial cycles of freezing–defreezing over several months.

Stock Solutions of Library Compounds. Whenever possible, 110 mM stock solutions of the library compounds were prepared in DMSO-*d*₆. These stocks were conserved at 4 °C without apparent degradation over at least 4 months. For NMR analyses, appropriate volumes of stock solutions were diluted to 500 μL samples with or without protein in phosphate-buffered H₂O. A 50 μL portion of D₂O was also added for deuterium lock. Thus, a final concentration of 1 mM for each screening compound could be obtained from 5 μL of stock solution (0.9% DMSO-*d*₆ in the final sample, with no

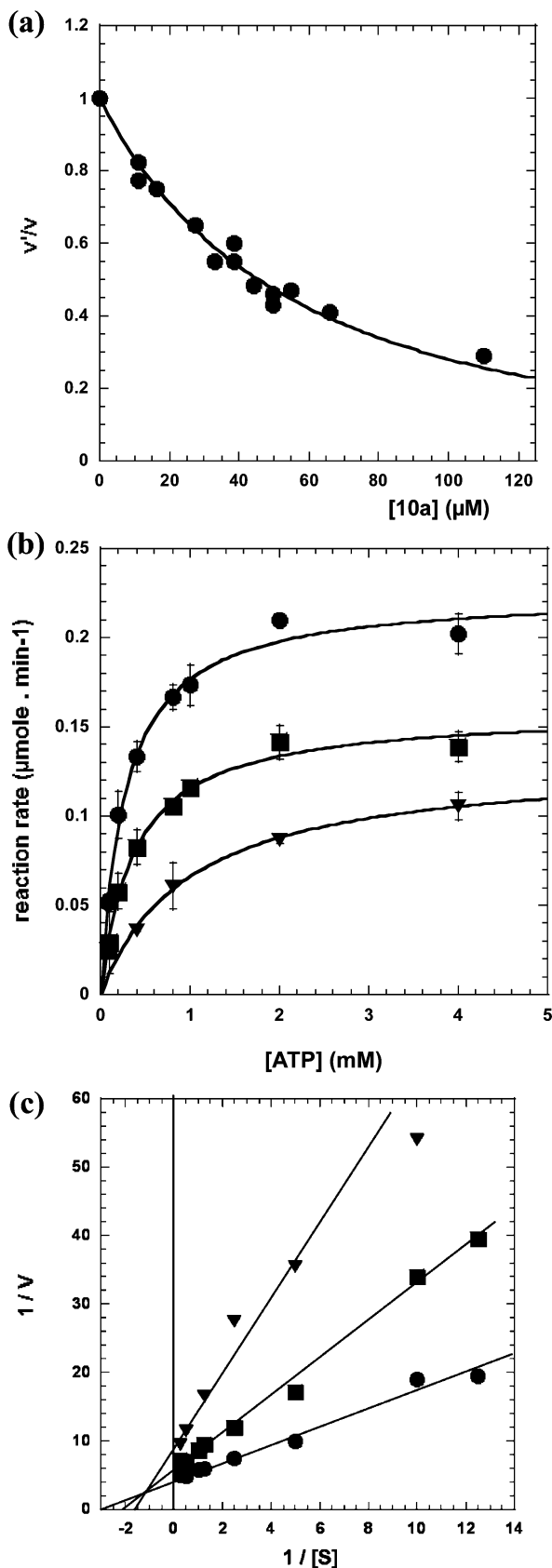


Figure 5. (a) Inhibition of CK as a function of inhibitor (10a) concentration, plotted as the ratio of the reaction rate in the presence of 10a (v') to the uninhibited reaction rate (v). (b) Reaction rates versus MgATP concentration in the absence (●) or with 27.5 μM (■) and 55 μM (▼) compound 10a. Lines correspond to a fit to a mixed type of reversible inhibition. (c) Corresponding Lineweaver–Burk plots.

effect on CK reactivity, data not shown). In a few cases, the stock solutions were further diluted in $\text{DMSO-}d_6$ owing to reduced solubility in either $\text{DMSO-}d_6$ or H_2O .

NMR Experiments. All spectra were acquired at 293 K with a Varian Inova 600 MHz NMR spectrometer, equipped with a standard 5 mm triple-resonance inverse probe with a z-axis field gradient, actively shielded, and with an autosampler robot. Control 1D ^1H spectra preceded all experiments to assess the purity and state of the analytes. Water suppression was achieved by a double spin–echo scheme²⁶ with 2.4 ms water-selective 180° square pulses. Spin locks (3.6 kHz) of 15 ms were also used after the detection pulse in every experiment to achieve protein suppression. The acquisition time was 1 s, the sweep width 12 ppm, and the relaxation delay 1.5 s. As for the processing, the data were zero-filled to 16000 complex points and multiplied by an exponential function (line broadening 0.3 Hz) prior to Fourier transformation. The same processing parameters and suppression schemes were also used with WaterLOGSY^{27,45} and STD^{46,47} sequences. In the WaterLOGSY experiment, the first water-selective 180° Gaussian pulse was 25 ms long, and a weak rectangular pulse field gradient was applied during the mixing time (1 s). A gradient recovery time of 2 ms was introduced after the mixing time; gradient recoveries were otherwise 200 ms long. The relaxation delay was 2 s. In the STD experiment, selective saturation of the protein at 2046 Hz from the carrier frequency was carried out by a 2 s pulse train (40 Gaussian pulses of 50 ms between 1 ms delays). A relaxation delay of 100 ms preceded each new scan. Each NMR screen consisted of 1D ^1H , STD, and WaterLOGSY experiments performed on mixtures of 2–6 compounds. Spectra were processed and analyzed with MestReC 4.4.1.0 (Mestrelab Research, Santiago de Compostella, Spain).

For quantitative analyses of STD spectra, the STD amplification factors f_{STD} were derived from the equation³⁸

$$f_{\text{STD}} = \frac{I_{\text{STD}}}{I_0} \frac{[\text{L}]_{\text{tot}}}{[\text{CK}]_{\text{tot}}}$$

where I_{STD} and I_0 are peak integrals in the STD or 1D experiment, respectively, and $[\text{L}]_{\text{tot}}$ and $[\text{CK}]_{\text{tot}}$ are the total concentrations of the ligand and CK, respectively. Dissociation constants (K_{D}) were determined from a plot of $[\text{L}]_{\text{tot}}$ vs f_{STD} fitted by nonlinear regression analysis using the Levenberg–Marquardt algorithm in OriginPro 7 (OriginLab).

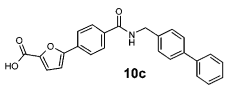
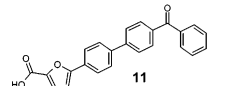
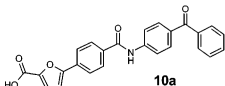
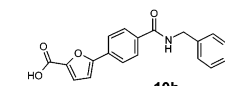
Quantitative LOGSY effects^{48,49} were measured as the relative percentage differences, $[(I_{\text{p}} - I_{\text{f}}) \times 100]/I_{\text{f}}$, between the NMR line intensities of a ligand in the presence (I_{p}) or the absence (I_{f}) of 10 μM CK. In the absence of binding the two intensities are equal, leading to a null LOGSY effect (0%).

Structural Models of CK Used for Ligand Docking. Structural models used for docking calculations were derived from the crystal structures of rabbit muscular CK available from the Protein Data Bank. The 2CRK entry⁵⁰ was chosen as a model for the open, substrate-free CK after reconstruction of the missing residues 323–331 with Modeller 8^{51–53} using the conformation of chain A of the 1VRP entry.³² Chain B of the 1U6R coordinates was chosen as a model for the closed, substrate-bound CK conformation since it is complexed with creatine, MgADP, and a nitrate ion mimicking a transition-state conformation.

Virtual Screening and Scoring. Prior to the docking process, the target protein and the ligands were subjected to slight modifications using the Sybyl software (Tripos, Inc.). All the hydrogens and charges in the protein were added, and their positions were energy minimized according to the Powell method. The different ligands were built using the Sybyl sketch tool. Several atom types were modified to account for their protonation states. Charges were computed according to the Gasteiger–Hückel method, and the ligand energy was minimized using the Tripos force field with the simplex method followed by the conjugate gradient method.

Ligand docking to the target receptor was performed with the DOCK 5.4 software package.⁵⁰ After molecular surface calculation,

Table 3. Ranking of the Synthesized Follow-Ups Based on Enzymatic Assays (Middle Column)^a

Inhibitor	% inhibition	DOCK energy (kcal/mol)	Additional data ^b
	63	-51,8	clogP = 5.44, M _w = 397.43
	63	-46,3	clogP = 5.68, M _w = 368.39
	35	-49,5	clogP = 4.62, M _w = 411.42 K _i = 25 ± 5 μM, αK _i = 70 ± 4 μM
	20	-47,4	clogP = 3.68, M _w = 321.34

^a The results of docking calculations are added for comparison (right column) and show a good overall agreement. Inhibition constants of **10a** against free CK (K_i) and the complex CK–MgATP (αK_i) are indicated (see the text). ^b $c \log P$ values correspond to predicted partition coefficient values, obtained from the KowWin software (Syracuse Research Corp.).⁴⁴ M_w is the weight-average molar mass (g/mol).

the potential interaction sites were filled with spheres to map their locations. Only those spheres within the binding pockets of ADP and creatine were retained as relevant for further computation. As an outcome, 170 spheres were selected for the closed conformation whereas 207 spheres were retained for the open conformation prior to grid energy computation. The corresponding grid was chosen to enclose the selected spheres plus an extra margin of 2 Å. We resorted to the anchor-first search method with an “anchor size” of 6 to account for several anchor fragments, whereas other ligand flexibility parameters were assigned their standard default values. A total of 50 configurations per ligand building cycle and a maximum of 5000 orientations were generated. The docked ligands were ranked according to their energy scores since this was previously reported as the most robust method.^{54,55} Moreover, we considered here the mean energy score between the runs with open and closed conformations. Three different values of the seeds were used as recommended previously.³⁰ The highest deviation in terms of energy score was 1.5 kcal/mol by considering all the ligands. The latter value did not alter the final ranking of the complete set of ligands.

Virtual Follow-Up of the Hits. Follow-up compounds of the first NMR hit were built in three steps using the Ilib Diverse 1.02 software (Inte:Ligand Software-Entwicklungs-und Consulting GmbH, Maria Enzersdorf, Austria). On one hand, a few derivatives of **1** with varying linker types and lengths, added to the phenyl ring, were constructed. The linkers were one, two, or three atoms long (C or N) and positioned *meta* or *para* with regard to the furan ring (see Table 2). The structure of compound **1** was also used as is. On the other hand, a list of potential substituents was selected, either from the list of NMR hits or from a set of the Ilib Diverse default library (aniline, anisole, benzene, 1-benzofuran, benzophenone, diphenyl, furane, imidazole, indole, isoquinoline, naphthalene, pyridine, pyrrole, quinoline). Finally the **1**-related motifs and the precited substituents were randomly paired using the Ilib Diverse software. A Lipinski-compliant filter was applied to select potential candidates: $M_w \leq 500 \text{ g}\cdot\text{mol}^{-1}$, a maximum of 10 H bond acceptors and 5 H bond donors, $c \log P$ between -3.5 and 5 , and number of rings ≤ 4 . A total of 1000 molecules were generated. A 3D conformation for each compound was readily obtained from the Ilib Diverse software, which uses CORINA (Molecular Networks GmbH, Erlangen, Germany). The output was an SDF file, converted into a mol2 file using OpenBabel for subsequent virtual screening with DOCK.

Chemistry. General Methods. Thin-layer chromatography (TLC) was carried out on aluminum sheets coated with silica gel 60 F (Merck 5554). TLC plates were inspected by UV light and developed by treatment with a mixture of 5% H₂SO₄ in EtOH followed by heating. Silica gel column chromatography was performed with Geduran silica gel Si 60 (40–63 μm) purchased from Merck (Darmstadt, Germany). ¹H and ¹³C NMR spectra were recorded using Bruker AC200 and DRX300 spectrometers with the residual solvent as the internal standard. The following abbreviations are used to explain the observed multiplicities: s, singlet; d, doublet; dd, doublet of doublets; ddd, doublet of doublets of doublets; t, triplet; m, multiplet. NMR solvents were purchased from Eurisotop (Saint Aubin, France). HRMS (LSIMS, CI) mass spectra were recorded in the positive mode (unless stated otherwise) using a Thermo Finnigan Mat 95 XL spectrometer. Elemental analyses were carried out by the Service de Microanalyses du CNRS, Division de Vernaison, France.

tert-Butyl 5-Bromofuran-2-carboxylate (6). To a suspension of MgSO₄ (1.8 g, 15 mmol) in CH₂Cl₂ (28 mL) was added H₂SO₄ (384 μL, 7.5 mmol). The mixture was stirred at room temperature for 15 min, and 5-bromo-2-furoic acid (1.37 g, 7.1 mmol) and tBuOH (3.4 mL, 35 mmol) were introduced. The mixture was stirred at room temperature for 48 h. The reaction was quenched with saturated aqueous NaHCO₃ and diluted with CH₂Cl₂. The organic layer was washed with brine, dried over Na₂SO₄, filtered, and concentrated to dryness to afford **6** (1.03 g, 55%) as a yellow oil: ¹H NMR (300 MHz, CDCl₃) δ 6.98 (d, 1H, $J = 3.5$ Hz, H_{furan}), 6.38 (d, 1H, $J = 3.5$ Hz, H_{furan}), 1.54 (s, 9H, tBu); ¹³C NMR (75 MHz, CDCl₃) δ 162.2 (C=O), 147.4 (C₂), 126.5 (CBr), 119.0, 113.5 (C₃, C₄), 82.3 (C(CH₃)₃), 28.1 (C(CH₃)₃); MS (EI) m/z 246 [M]⁺; HRMS (EI) m/z calcd for C₉H₁₁BrO₃ 245.9892, found 245.9887.

4-[5-(tert-Butoxycarbonyl)-2-furyl]benzoic Acid (7). To a solution of **6** (1.03 g, 3.9 mmol) in 1,4-dioxane (150 mL) was added Pd(PPh₃)₄ (226 mg, 0.19 mmol). The mixture was stirred at room temperature for 15 min, and 4-carboxyphenylboronic acid (649 mg, 3.9 mmol), dissolved in water (37 mL), and K₂CO₃ (1.08 g, 7.8 mmol) were introduced. The mixture was stirred at 100 °C for 16 h. The reaction was filtered through a Celite pad, and the solvent was removed under vacuum. The residue was diluted in EtOAc and washed with water. The aqueous layer was acidified to pH 6 and extracted with EtOAc. The organic layer was dried over Na₂SO₄, filtered, and concentrated to dryness to afford **7** (826 mg, 74%) as a white solid: ¹H NMR (300 MHz, MeOD) δ 8.05 (d, 2H, $J =$

8.3 Hz, H_{arom}), 7.85 (d, 2H, $J = 8.3$ Hz, H_{arom}), 7.17 (d, 1H, $J = 3.5$ Hz, H_{furan}), 7.02 (d, 1H, $J = 3.5$ Hz, H_{furan}), 1.57 (s, 9H, tBu); ^{13}C NMR (75 MHz, MeOD) δ 169.1 (COOH), 159.6 (COOtBu), 157.3 (C_5), 146.7 (C_2), 134.7 (C_9), 131.8 (C_6), 131.4, 125.4 (C_7 , C_8 , C_{10} , C_{11}), 120.4, 110.0 (C_3 , C_4), 83.4 ($\text{C}(\text{CH}_3)_3$), 28.4 ($\text{C}(\text{CH}_3)_3$); MS (EI) m/z 288 $[\text{M}]^+$; HRMS (EI) m/z calcd for $\text{C}_{16}\text{H}_{16}\text{O}_5$ 288.0998, found 288.0994. Anal. Calcd for $\text{C}_{16}\text{H}_{16}\text{O}_5 \cdot 0.4\text{H}_2\text{O}$: C, 65.03; H, 5.73. Found: C, 65.09; H, 5.56.

General Procedure for the Synthesis of Amides 9a–c. Carboxylic acid **7** (1 equiv) was azeotropically evaporated two times with toluene and dissolved in DMF (1 mL). Oxalyl chloride (2 M in CH_2Cl_2 , 2 mL) was added to the mixture. The reaction was stirred at room temperature for 16 h, and the solvent was removed in vacuo to afford **8**. Acyl chloride **8** (1 equiv) was dissolved in pyridine (1 mL), and the appropriate amine (1.02 equiv) was added. The mixture was stirred at room temperature for 1 h. The reaction was diluted in CH_2Cl_2 and washed with water. The organic layer was dried over Na_2SO_4 , filtered, and concentrated to dryness. Purification (SiO_2 , 0–50% gradient of EtOAc in CH_2Cl_2) afforded **9a–c** as white solids.

Data for tert-butyl 5-(4-[[benzoylphenyl]amino]carbonyl)-phenyl)-2-furoate (9a): yield 72%; ^1H NMR (300 MHz, CDCl_3) δ 8.96 (br s, 1H, NH), 7.84–7.80 (m, 4H, H_{arom}), 7.73–7.58 (m, 6H, H_{arom}), 7.50–7.45 (m, 1H, H_{arom}), 7.39–7.34 (m, 2H, H_{arom}), 7.02 (d, 1H, $J = 3.5$ Hz, H_{furan}), 6.67 (d, 1H, $J = 3.5$ Hz, H_{furan}), 1.50 (s, 9H, tBu); ^{13}C NMR (75 MHz, CDCl_3) δ 196.4 (CO), 166.1 (CONH), 158.6 (COOtBu), 155.9 (C_5), 145.9 (C_2), 142.8, 138.1, 134.5 (C_{13} , C_{16} , C_{20}), 133.4, 133.0 (C_6 , C_9), 132.7, 131.9, 130.3, 128.7, 128.3, 125.0, 120.0 (C_7 , C_8 , C_{10} , C_{11} , C_{14} , C_{15} , C_{17} , C_{18} , C_{21} , C_{22} , C_{23} , C_{24} , C_{25}), 119.5, 108.8 (C_3 , C_4), 82.7 ($\text{C}(\text{CH}_3)_3$), 28.6 ($\text{C}(\text{CH}_3)_3$). Anal. Calcd for $\text{C}_{29}\text{H}_{25}\text{NO}_5 \cdot 0.05\text{CH}_2\text{Cl}_2$: C, 73.68; H, 5.38; N, 2.96. Found: C, 73.44; H, 5.39; N, 2.91.

Data for tert-butyl 5-(4-[[benzylamino]carbonyl]phenyl)-2-furoate (9b): yield 87%; ^1H NMR (300 MHz, CDCl_3) δ 7.74 (m, 4H, H_{arom}), 7.29–7.25 (m, 5H, H_{arom}), 7.06 (d, 1H, $J = 3.5$ Hz, H_{furan}), 6.71 (d, 1H, $J = 3.5$ Hz, H_{furan}), 6.47 (br s, 1H, NH), 4.57 (d, 2H, $J = 5.6$ Hz, CH_2), 1.52 (s, 9H, tBu); ^{13}C NMR (75 MHz, CDCl_3) δ 167.0 (CONH), 158.4 (COOtBu), 156.0 (C_5), 145.9 (C_2), 138.4 (C_{14}), 134.2, 132.8 (C_6 , C_9), 129.2, 128.3, 128.0, 127.9, 125.0 (C_7 , C_8 , C_{10} , C_{11} , C_{15} , C_{16} , C_{17} , C_{18} , C_{19}), 119.3, 108.5 (C_3 , C_4), 82.5 ($\text{C}(\text{CH}_3)_3$), 44.6 (CH_2), 28.6 ($\text{C}(\text{CH}_3)_3$). Anal. Calcd for $\text{C}_{23}\text{H}_{23}\text{NO}_4$: C, 73.19; H, 6.14; N, 3.71. Found: C, 72.63; H, 6.18; N, 3.74.

Data for tert-butyl 5-(4-[[biphenyl-4-ylmethyl]amino]carbonyl)-phenyl)-2-furoate (9c): yield 39%; ^1H NMR (300 MHz, CDCl_3) δ 7.85 (q, 4H, $J = 8.6$ Hz, H_{arom}), 7.58–7.13 (m, 9H, H_{arom}), 7.06 (d, 1H, $J = 3.5$ Hz, H_{furan}), 6.71 (d, 1H, $J = 3.5$ Hz, H_{furan}), 6.47 (br s, 1H, NH), 4.68 (d, 2H, $J = 5.6$ Hz, CH_2), 1.58 (s, 9H, tBu); ^{13}C NMR (75 MHz, CDCl_3) δ 162.2 (CONH), 157.4 (COOtBu), 155.6 (C_5), 145.5 (C_2), 140.6, 140.5 (C_{17} , C_{20}), 137.0 (C_{14}), 133.9, 132.3 (C_6 , C_9), 128.7, 128.3, 127.5, 127.4, 127.3, 127.0, 124.6 (C_7 , C_8 , C_{10} , C_{11} , C_{15} , C_{16} , C_{18} , C_{19} , C_{21} , C_{22} , C_{23} , C_{24} , C_{25}), 118.8, 108.1 (C_3 , C_4), 82.0 ($\text{C}(\text{CH}_3)_3$), 43.8 (CH_2), 28.2 ($\text{C}(\text{CH}_3)_3$). Anal. Calcd for $\text{C}_{29}\text{H}_{27}\text{NO}_4$: C, 76.80; H, 6.00; N, 3.09. Found: C, 77.14; H, 6.24; N, 2.97.

General Procedure for the Synthesis of Acids 10a–c. Compounds **9a–c** (1 equiv) were dissolved in CH_2Cl_2 (1 mL), and TFA (600 μL) was added. The mixture was stirred at room temperature for 1 h, and the solvent was removed in vacuo to afford **10a–c** as white solids.

Data for 5-(4-[[benzoylphenyl]amino]carbonyl)phenyl)-2-furoic acid (10a): yield 95%; ^1H NMR (300 MHz, $\text{DMSO}-d_6$) δ 10.69 (br s, 1H, NH), 8.10 (d, 2H, $J = 8.6$ Hz, H_{arom}), 7.99, 7.96 (2d, 4H, $J = 7.2$ Hz, H_7 , H_8 , H_{10} , H_{11}), 7.80–7.50 (m, 7H, H_{arom}), 7.35 (d, 1H, $J = 3.6$ Hz, H_{furan}), 7.32 (d, 1H, $J = 3.5$ Hz, H_{furan}); ^{13}C NMR (75 MHz, $\text{DMSO}-d_6$) δ 195.5 (C_{19}), 166.1 (CONH), 160.0 (COOH), 156.0 (C_5), 145.7 (C_2), 144.1, 138.3, 135.1 (C_{13} , C_{16} , C_{20}), 133.1, 132.9 (C_6 , C_9), 132.6, 131.8, 130.2, 129.6, 129.3, 125.0, 120.4 (C_7 , C_8 , C_{10} , C_{11} , C_{14} , C_{15} , C_{17} , C_{18} , C_{21} , C_{22} , C_{23} , C_{24} , C_{25}), 120.7, 110.6 (C_3 , C_4). Anal. Calcd for $\text{C}_{25}\text{H}_{17}\text{NO}_5 \cdot 0.1\text{H}_2\text{O}$: C, 72.67; H, 4.20; N, 3.39. Found: C, 72.35; H, 4.30; N, 3.30.

Data for 5-(4-[[benzylamino]carbonyl]phenyl)-2-furoic acid (10b): yield 46%; ^1H NMR (300 MHz, $\text{DMSO}-d_6$) δ 9.14 (t, 1H, H_7 , H_{10} , H_{11}), 8.01, 7.91 (2d, 4H, $J = 8.4$ Hz, $J = 8.4$ Hz, H_7 , H_8 , H_{10} , H_{11}), 7.35–7.23 (m, 7H, H_3 , H_4 , H_{15} , H_{16} , H_{17} , H_{18} , H_{19}), 4.50 (d, 2H, $J = 5.9$ Hz, CH_2); ^{13}C NMR (75 MHz, $\text{DMSO}-d_6$) δ 166.3 (CONH), 160.0 (COOH), 156.2 (C_5), 145.6 (C_2), 140.4 (C_{14}), 135.0, 132.3 (C_6 , C_9), 129.1, 125.0 (C_7 , C_8 , C_{10} , C_{11}), 128.9, 128.1, 127.6, 125.0 (C_{15} , C_{16} , C_{17} , C_{18} , C_{19}), 120.6, 110.2 (C_3 , C_4), 43.5 (CH_2). Anal. Calcd for $\text{C}_{19}\text{H}_{15}\text{NO}_4 \cdot 0.1\text{H}_2\text{O}$: C, 70.62; H, 4.74; N, 4.33. Found: C, 70.43; H, 4.78; N, 4.33.

Data for 5-(4-[[biphenyl-4-ylmethyl]amino]carbonyl)phenyl)-2-furoic acid (10c): yield 90%; ^1H NMR (300 MHz, $\text{DMSO}-d_6$) δ 9.18 (t, 1H, $J = 5.8$ Hz, NH), 8.03, 7.92 (2d, 4H, $J = 8.3$ Hz, $J = 8.3$ Hz, H_7 , H_8 , H_{10} , H_{11}), 7.65–7.62 (m, 4H, H_{arom}), 7.48–7.28 (m, 7H, H_3 , H_4 , H_{arom}), 4.54 (d, 2H, $J = 5.3$ Hz, CH_2); ^{13}C NMR (75 MHz, $\text{DMSO}-d_6$) δ 166.3 (CONH), 160.0 (COOH), 156.2 (C_5), 145.5 (C_2), 140.8, 139.7, 139.6 (C_{14} , C_{17} , C_{20}), 135.0, 132.3 (C_6 , C_9), 129.7, 128.9, 128.7, 128.1, 127.5, 127.4, 125.0 (C_7 , C_8 , C_{10} , C_{11} , C_{15} , C_{16} , C_{18} , C_{19} , C_{21} , C_{22} , C_{23} , C_{24} , C_{25}), 120.7, 110.2 (C_3 , C_4), 43.2 (CH_2). Anal. Calcd for $\text{C}_{25}\text{H}_{19}\text{NO}_4 \cdot 1.2\text{H}_2\text{O}$: C, 71.63; H, 5.15; N, 3.34. Found: C, 71.24; H, 4.68; N, 3.22.

5-(4'-Benzoylbiphenyl-4-yl)-2-furoic Acid (11). To a solution of 5-(4-bromophenyl)-2-furoic acid (1 equiv) in 1,4-dioxane (8 mL/0.20 mmol) was added Pd(PPh_3)₄ (0.05 equiv). The mixture was stirred at room temperature for 15 min, and 4-benzoylphenylboronic acid (1 equiv), dissolved in water (2 mL), and K_2CO_3 (2 equiv) were introduced. The mixture was stirred at 100 °C for 16 h. The reaction was filtered through a Celite pad, and the solvent was removed under vacuum. The residue was diluted in EtOAc and washed with water. The aqueous layer was acidified to pH 6 and washed with EtOAc. The organic layer was dried over Na_2SO_4 , filtered, and concentrated to dryness to afford **11** as a white solid; yield 10%; ^1H NMR (300 MHz, $\text{DMSO}-d_6$) δ 7.97–7.68 (m, 11H, H_{arom}), 7.62–7.57 (m, 2H, H_{arom}), 7.35 (d, 1H, $J = 3.6$ Hz, H_{furan}), 7.25 (d, 1H, $J = 3.6$ Hz, H_{furan}); ^{13}C NMR (75 MHz, $\text{DMSO}-d_6$) δ 196.1 (C_{18}), 160.1 (COOH), 156.5 (C_5), 145.3 (C_2), 144.0, 138.8, 138.0, 136.8, 133.5 (C_6 , C_9 , C_{12} , C_{15} , C_{19}), 133.5, 131.3, 130.4, 129.4, 128.5, 127.5, 125.9 (C_7 , C_8 , C_{10} , C_{11} , C_{13} , C_{14} , C_{16} , C_{17} , C_{20} , C_{21} , C_{22} , C_{23} , C_{24}), 120.7, 109.4 (C_3 , C_4). Anal. Calcd for $\text{C}_{24}\text{H}_{16}\text{O}_4 \cdot 1.2\text{H}_2\text{O}$: C, 73.91; H, 4.76. Found: C, 73.93; H, 4.67.

Biological Activity. The activity of CK was measured using the pH-stat method in the forward reaction $\text{MgATP} + \text{creatine} \rightarrow \text{MgADP} + \text{phosphocreatine} + \text{H}^+$.⁵⁶ The reaction rate was deduced from the rate of 10^{-2} M NaOH addition necessary to maintain a constant pH of 8.8 at 30 °C. The CK concentration was kept at 10 nM in 2.0 mL of assay medium containing 4 mM MgATP and 40 mM creatine ($K_M^{\text{Cr}} = 6.1$ mM). When variable, MgATP concentrations ranged from 0.08 to 4.00 mM, magnesium was added as magnesium acetate and always kept in a 1 mM excess over the MgATP complex. A 5 or 10 μL portion of an 11 mM $\text{DMSO}-d_6$ stock solution of **10a** (27.5 or 55 μM final concentration) was incubated for 3 min in the assay medium (containing CK and creatine) before the reaction was started by ATP addition (DMSO by itself had no effect on the CK reaction rate). The Michaelis constant K_M was obtained by fitting the substrate-dependent reaction velocities to the rate equation for a rapid equilibrium random mechanism:

$$v = \frac{V_m * [S]}{K_M * \left(1 + \frac{[I]}{K_I}\right) + [S] * \left(1 + \frac{[I]}{\alpha K_I}\right)}$$

For the ranking of the different follow-up compounds (**10a–c** and **11**) a single experiment at 400 μM MgATP was performed either without (reference experiment) or with the tested molecule at 27.5 μM .

Acknowledgment. A.-S.B. is the recipient of a doctoral fellowship from Région Rhône-Alpes (France), which also supported this work by a grant in aid 2003–2006 (NTAM

Projects 04-022-408-01 and 05-01-900-701). Support from the European Union, Contract No. LSHB-CT-2004-503467, to P.G. and A.J. is gratefully acknowledged. We are also grateful to the Institut du Développement et des Ressources en Informatique Scientifique (IDRIS), CNRS, France, for use of its supercomputing facility. We gratefully acknowledge Inte:Ligand Software-Entwicklungs-und Consulting GmbH, Maria Enzersdorf, Austria, for providing us with a test copy of the Ilib Diverse 1.02 software. We finally thank Dr. Jonathan Moore for helpful guidelines regarding the NMR library generation.

References

- MacCoss, M.; Baillie, T. A. Organic chemistry in drug discovery. *Science* **2004**, *303*, 1810–1813.
- Rees, D. C.; Congreve, M.; Murray, C. W.; Carr, R. Fragment-based lead discovery. *Nat. Rev. Drug Discovery* **2004**, *3*, 660–672.
- Lepre, C. A.; Peng, J.; Fejzo, J.; Abdul-Manan, N.; Pocas, J.; Jacobs, M.; Xie, X.; Moore, J. M. Applications of SHAPES screening in drug discovery. *Comb. Chem. High Throughput Screening* **2002**, *5*, 583–590.
- Sem, D. S.; Bertolaet, B.; Baker, B.; Chang, E.; Costache, A. D.; Coutts, S.; Dong, Q.; Hansen, M.; Hong, V.; Huang, X.; Jack, R. M.; Kho, R.; Lang, H.; Ma, C. T.; Meininger, D.; Pellicchia, M.; Pierre, F.; Villar, H.; Yu, L. Systems-based design of bi-ligand inhibitors of oxidoreductases: filling the chemical proteomic toolbox. *Chem. Biol.* **2004**, *11*, 185–194.
- Shuker, S. B.; Hajduk, P. J.; Meadows, R. P.; Fesik, S. W. Discovering high-affinity ligands for proteins: SAR by NMR. *Science* **1996**, *274*, 1531–1534.
- Oprea, T. I.; Davis, A. M.; Teague, S. J.; Leeson, P. D. Is there a difference between leads and drugs? A historical perspective. *J. Chem. Inf. Comput. Sci.* **2001**, *41*, 1308–1315.
- Carr, R. A.; Congreve, M.; Murray, C. W.; Rees, D. C. Fragment-based lead discovery: leads by design. *Drug Discovery Today* **2005**, *10*, 987–992.
- Boehm, H. J.; Boehringer, M.; Bur, D.; Gmuender, H.; Huber, W.; Klaus, W.; Kostrewa, D.; Kuehne, H.; Luebbbers, T.; Meunier-Keller, N.; Mueller, F. Novel inhibitors of DNA gyrase: 3D structure based biased needle screening, hit validation by biophysical methods, and 3D guided optimization. A promising alternative to random screening. *J. Med. Chem.* **2000**, *43*, 2664–2674.
- Teague, S. J.; Davis, A. M.; Leeson, P. D.; Oprea, T. The Design of Leadlike Combinatorial Libraries. *Angew. Chem., Int. Ed.* **1999**, *38*, 3743–3748.
- Congreve, M.; Carr, R.; Murray, C.; Jhoti, H. A 'rule of 3' for fragment-based lead discovery? *Drug Discovery Today* **2003**, *8*, 876–877.
- Diercks, T.; Coles, M.; Kessler, H. Applications of NMR in drug discovery. *Curr. Opin. Chem. Biol.* **2001**, *5*, 285–291.
- Peng, J. W.; Moore, J.; Abdul-Manan, N. NMR experiments for lead generation in drug discovery. *Prog. Nucl. Magn. Reson. Spectrosc.* **2004**, *44*, 225–256.
- Fielding, L.; Fletcher, D.; Rutherford, S.; Kaur, J.; Mestres, J. Exploring the active site of human factor Xa protein by NMR screening of small molecule probes. *Org. Biomol. Chem.* **2003**, *1*, 4235–4241.
- Becattini, B.; Sareth, S.; Zhai, D.; Crowell, K. J.; Leone, M.; Reed, J. C.; Pellicchia, M. Targeting apoptosis via chemical design: inhibition of bid-induced cell death by small organic molecules. *Chem. Biol.* **2004**, *11*, 1107–1117.
- Fejzo, J.; Lepre, C. A.; Peng, J. W.; Bemis, G. W.; Ajay, Murcko, M. A.; Moore, J. M. The SHAPES strategy: an NMR-based approach for lead generation in drug discovery. *Chem. Biol.* **1999**, *6*, 755–769.
- Baurin, N.; Aboul-Ela, F.; Barril, X.; Davis, B.; Drysdale, M.; Dymock, B.; Finch, H.; Fromont, C.; Richardson, C.; Simmonite, H.; Hubbard, R. E. Design and characterization of libraries of molecular fragments for use in NMR screening against protein targets. *J. Chem. Inf. Comput. Sci.* **2004**, *44*, 2157–2166.
- Hajduk, P. J.; Bures, M.; Praestgaard, J.; Fesik, S. W. Privileged molecules for protein binding identified from NMR-based screening. *J. Med. Chem.* **2000**, *43*, 3443–3447.
- Lepre, C. A. Library design for NMR-based screening. *Drug Discovery Today* **2001**, *6*, 133–140.
- Bemis, G. W.; Murcko, M. A. The properties of known drugs. 1. Molecular frameworks. *J. Med. Chem.* **1996**, *39*, 2887–2893.
- Bemis, G. W.; Murcko, M. A. Properties of known drugs. 2. Side chains. *J. Med. Chem.* **1999**, *42*, 5095–5099.
- McLeish, M. J.; Kenyon, G. L. Relating structure to mechanism in creatine kinase. *Crit. Rev. Biochem. Mol. Biol.* **2005**, *40*, 1–20.
- Wallimann, T.; Wyss, M.; Brdiczka, D.; Nicolay, K.; Eppenberger, H. M. Intracellular compartmentation, structure and function of creatine kinase isoenzymes in tissues with high and fluctuating energy demands: the 'phosphocreatine circuit' for cellular energy homeostasis. *Biochem. J.* **1992**, *281* (Part 1), 21–40.
- Wyss, M.; Kaddurah-Daouk, R. Creatine and creatinine metabolism. *Physiol. Rev.* **2000**, *80*, 1107–1213.
- Pereira, C. A.; Alonso, G. D.; Ivaldi, S.; Bouvier, L. A.; Torres, H. N.; Flawia, M. M. Screening of substrate analogs as potential enzyme inhibitors for the arginine kinase of *Trypanosoma cruzi*. *J. Eukaryotic Microbiol.* **2003**, *50*, 132–134.
- Min, K. L.; Steghens, J. P.; Henry, R.; Doutheau, A.; Collombel, C. N-dibenzylphospho-N'-3-(2,6-dichlorophenyl)propyl-guanidine is a bisubstrate-analog for creatine kinase. *Biochim. Biophys. Acta* **1997**, *1342*, 83–89.
- Hwang, T. L.; Shaka, A. J. Water suppression that works—Excitation sculpting using arbitrary wave-forms and pulsed-field gradients. *J. Magn. Reson., A* **1995**, *112*, 275–279.
- Dalvit, C.; Fogliatto, G.; Stewart, A.; Veronesi, M.; Stockman, B. WaterLOGSY as a method for primary NMR screening: practical aspects and range of applicability. *J. Biomol. NMR* **2001**, *21*, 349–359.
- Fielding, L.; Rutherford, S.; Fletcher, D. Determination of protein-ligand binding affinity by NMR: observations from serum albumin model systems. *Magn. Reson. Chem.* **2005**, *43*, 463–470.
- Jencks, W. P. On the attribution and additivity of binding energies. *Proc. Natl. Acad. Sci. U.S.A.* **1981**, *78*, 4046–4050.
- Ewing, T. J.; Makino, S.; Skillman, A. G.; Kuntz, I. D. DOCK 4.0: search strategies for automated molecular docking of flexible molecule databases. *J. Comput.-Aided Mol. Des.* **2001**, *15*, 411–428.
- Forstner, M.; Kriechbaum, M.; Laggner, P.; Wallimann, T. Structural changes of creatine kinase upon substrate binding. *Biophys. J.* **1998**, *75*, 1016–1023.
- Lahiri, S. D.; Wang, P. F.; Babbitt, P. C.; McLeish, M. J.; Kenyon, G. L.; Allen, K. N. The 2.1 Å structure of Torpedo californica creatine kinase complexed with the ADP-Mg(2+)-NO(3)(-)-creatine transition-state analogue complex. *Biochemistry* **2002**, *41*, 13861–13867.
- Lipinski, C. A.; Lombardo, F.; Dominy, B. W.; Feeney, P. J. Experimental and computational approaches to estimate solubility and permeability in drug discovery and development settings. *Adv. Drug Delivery Rev.* **2001**, *46*, 3–26.
- Wright, S. W.; Hageman, D. L.; Wright, A. S.; McClure, L. D. Convenient preparations of t-butyl esters and ethers from t-butanol. *Tetrahedron Lett.* **1997**, *38*, 7345–7348.
- Jiang, W.; Sui, Z.; Macielag, M. J.; Walsh, S. P.; Fiordeliso, J. J.; Lanter, J. C.; Guan, J.; Qiu, Y.; Kraft, P.; Bhattacharjee, S.; Craig, E.; Haynes-Johnson, D.; John, T. M.; Clancy, J. Furoyl and benzofuroyl pyrroloquinolones as potent and selective PDE5 inhibitors for treatment of erectile dysfunction. *J. Med. Chem.* **2003**, *46*, 441–444.
- Jung, J. H.; Rim, J. A.; Han, W. S.; Lee, S. J.; Lee, Y. J.; Cho, E. J.; Kim, J. S.; Ji, Q.; Shimizu, T. Hydrogel behavior of a sugar-based gelator by introduction of an unsaturated moiety as a hydrophobic group. *Org. Biomol. Chem.* **2006**, *4*, 2033–2038.
- Byran, D. B.; Hall, R. F.; Holden, K. G.; Huffman, W. F.; Gleason, J. G. Nuclear analogues of beta-lactam antibiotics. 2 The total synthesis of 8-oxo-4-thia-z-azabicyclo[4.2.0]oct-2-ene-2-carboxylic acids. *J. Am. Chem. Soc.* **1977**, *99*, 2353–2355.
- Meinecke, R.; Meyer, B. Determination of the binding specificity of an integral membrane protein by saturation transfer difference NMR: RGD peptide ligands binding to integrin $\alpha_{\text{IIb}}\beta_3$. *J. Med. Chem.* **2001**, *44*, 3059–3065.
- Hagemann, H.; Marcillat, O.; Buchet, R.; Vial, C. Magnesium-adenosine diphosphate binding sites in wild-type creatine kinase and in mutants: Role of aromatic residues probed by Raman and infrared spectroscopies. *Biochemistry* **2000**, *39*, 9251–9256.
- Segel, I. H. *Enzyme Kinetics: Behavior and Analysis of Rapid Equilibrium and Steady-State Enzyme Systems*; Wiley-Interscience: New York, 1975.
- Sobolev, V.; Sorokine, A.; Prilusky, J.; Abola, E. E.; Edelman, M. Automated analysis of interatomic contacts in proteins. *Bioinformatics* **1999**, *15*, 327–332.
- Pereira, C. A.; Alonso, G. D.; Ivaldi, S.; Silber, A.; Alves, M. J.; Bouvier, L. A.; Flawia, M. M.; Torres, H. N. Arginine metabolism in *Trypanosoma cruzi* is coupled to parasite stage and replication. *FEBS Lett.* **2002**, *526*, 111–114.
- Peng, J. W.; Lepre, C. A.; Fejzo, J.; Abdul-Manan, N.; Moore, J. M. Nuclear magnetic resonance-based approaches for lead generation in drug discovery. *Methods Enzymol.* **2001**, *338*, 202–230.
- Meylan, W. M.; Howard, P. H. Atom/fragment contribution method for estimating octanol-water partition coefficients. *J. Pharm. Sci.* **1995**, *84*, 83–92.

- (45) Dalvit, C.; Pevarello, P.; Tato, M.; Veronesi, M.; Vulpetti, A.; Sundstrom, M. Identification of compounds with binding affinity to proteins via magnetization transfer from bulk water. *J. Biomol. NMR* **2000**, *18*, 65–68.
- (46) Mayer, M.; Meyer, B. Characterization of ligand binding by saturation transfer difference NMR spectroscopy. *Angew. Chem., Int. Ed.* **1999**, *38*, 1784–1788.
- (47) Mayer, M.; Meyer, B. Group epitope mapping by saturation transfer difference NMR to identify segments of a ligand in direct contact with a protein receptor. *J. Am. Chem. Soc.* **2001**, *123*, 6108–6117.
- (48) Ciulli, A.; Williams, G.; Smith, A. G.; Blundell, T. L.; Abell, C. Probing hot spots at protein-ligand binding sites: A fragment-based approach using biophysical methods. *J. Med. Chem.* **2006**, *49*, 4992–5000.
- (49) Dalvit, C.; Fasolini, M.; Flocco, M.; Knapp, S.; Pevarello, P.; Veronesi, M. NMR-based screening with competition water-ligand observed via gradient spectroscopy experiments: Detection of high-affinity ligands. *J. Med. Chem.* **2002**, *45*, 2610–2614.
- (50) Rao, J. K.; Bujacz, G.; Wlodawer, A. Crystal structure of rabbit muscle creatine kinase. *FEBS Lett.* **1998**, *439*, 133–137.
- (51) Sali, A.; Blundell, T. L. Comparative protein modelling by satisfaction of spatial restraints. *J. Mol. Biol.* **1993**, *234*, 779–815.
- (52) Fiser, A.; Do, R. K.; Sali, A. Modeling of loops in protein structures. *Protein Sci.* **2000**, *9*, 1753–1773.
- (53) Marti-Renom, M. A.; Stuart, A. C.; Fiser, A.; Sanchez, R.; Melo, F.; Sali, A. Comparative protein structure modeling of genes and genomes. *Annu. Rev. Biophys. Biomol. Struct.* **2000**, *29*, 291–325.
- (54) Charifson, P. S.; Corkery, J. J.; Murcko, M. A.; Walters, W. P. Consensus scoring: A method for obtaining improved hit rates from docking databases of three-dimensional structures into proteins. *J. Med. Chem.* **1999**, *42*, 5100–5109.
- (55) Gohlke, H.; Hendlich, M.; Klebe, G. Knowledge-based scoring function to predict protein-ligand interactions. *J. Mol. Biol.* **2000**, *295*, 337–356.
- (56) Font, B.; Vial, C.; Goldschmidt, D.; Eichenberger, D.; Gautheron, D. C. Heart mitochondrial creatine kinase solubilization. Effect of mitochondrial swelling and SH group reagents. *Arch. Biochem. Biophys.* **1981**, *212*, 195–203.

JM061460R